



Dispersion of concentrated aqueous neodymia–yttria–alumina mixture with ammonium poly(acrylic acid) as dispersant

Yaohui Lv^{a,b}, Wei Zhang^a, Jie Tan^a, Yuanhua Sang^b, Haiming Qin^b, Jinlian Hu^a, Liuniu Tong^a, Hong Liu^{b,*}, Jiyang Wang^b, Robert I Boughton^c

^a School of Materials Science and Engineering, and Anhui Key Laboratory of Metal Materials and Processing, Anhui University of Technology, Anhui, Maanshan 243002, China

^b State Key Laboratory of Crystal Materials, Shandong University, 27 Shanda Nanlu, Jinan 250100, China

^c Department of Physics and Astronomy, Bowling Green State University, Bowling Green, OH 43403, USA

ARTICLE INFO

Article history:

Received 14 May 2010

Received in revised form 3 December 2010

Accepted 3 December 2010

Available online 13 December 2010

Keywords:

Oxide materials

Ceramics

Microstructure

Scanning electron microscopy

ABSTRACT

A stable aqueous slurry using ammonium polyacrylic acid polyelectrolyte as dispersant and a neodymia–yttria–alumina mixture was prepared as the starting powder. The effect of the polyelectrolyte concentration and the pH of the slurry on the stability of the suspension is studied, and the optimal pH value and the amount of dispersant needed to obtain a stable slurry were determined. Highly consistent slurries with optimal pH and dispersant concentration were prepared by ball milling. The rheological behavior of the slip with different solid loading (48–58 wt.%) has been studied by measuring the viscosity and shear stress as a function of shear rate. Slip with solid loadings of 53 wt.% shows near-Newtonian behavior but becomes non-Newtonian with typical shear-thinning behavior above this solid loading value. The density and microstructure of the cast product bears a direct relationship to the state of the slip induced by variation of the pH and the concentration of the dispersant as well as by solid loading. Transparent Nd:YAG ceramics were obtained by sintering of compacts prepared from optimized slurries at 1750 °C in vacuum.

© 2010 Elsevier B.V. All rights reserved.

1. Introduction

Transparent yttrium aluminum garnet ($\text{Y}_3\text{Al}_5\text{O}_{12}$) ceramic is an important laser material with excellent chemical stability, good optical and thermal properties, and high temperature creep resistance. It has proved to be one of the most promising laser materials for many kinds of laser devices, especially high power lasers [1–3]. Many factors, such as the purity of the raw materials, grain boundary thickness, ceramic porosity, etc., affect the transparency and laser properties of the ceramic. Among these factors, the number and size of micropores are the most important factors governing the optical and laser properties because of the scattering loss caused by the interface between the air in the pores and the ceramic substrate. Lowering the porosity of the ceramic is therefore the greatest challenge to improving the laser properties of YAG. Although there are three different YAG ceramic fabrication processes, including nanoparticle preparation, green body formation, and sintering, in attempting to control the porosity of the ceramic, the effect of the formation process is often ignored. The reported YAG formation methods are typically dry-pressing [4–10],

iso-static pressing [6,9,11,12] and a few reports that indicate using the slip casting method [13–16]. Generally speaking, using a green body obtained from a press formation method makes it difficult to obtain a pore-free ceramic with vacuum sintering because some air is always trapped in the closed micro-cavities formed by the tightly contacted particles in the green body during the high pressure formation process. It is difficult to pump out the trapped air in the furnace and so it forms micro-bubbles after vacuum sintering. It should be easier to obtain a dense ceramic formed with the slip casting method than with the press formation method because all the pores in the green body with the slip casting method originate from discharge channels in the dispersion medium. Therefore, the air in the connected channels can be more easily pumped out during vacuum sintering.

Based on this advantage, slip casting, which is an ancient formation method, has been intensively applied to the fabrication of transparent and other advanced ceramics, especially for multi-component systems and composites [17–21]. If the goal is the fabrication of pore-free transparent YAG ceramic, a uniform green body with high density is necessary. However, because the powder particles are of nanometer size, the slurry properties of the mixed powder are quite different from that in a clay suspension, a condition that presents a great obstacle to obtaining highly loaded slurries.

* Corresponding author. Tel.: +86 531 88362807.

E-mail address: hongliu@sdu.edu.cn (H. Liu).

As is well known, slip casting is based on a traditional formation process: a ceramic powder is dispersed in a dispersion medium, forms a slurry and is poured into a porous mold; the dispersion medium is expelled from the slurry under the capillary action of the mold, and a solid green body is obtained. The homogenization and the rheological behavior of the suspensions have been shown to play an important role in slip casting processing, and in turn, on the microstructure and other properties of the final product [13]. Therefore, the characteristics of the ceramic slurry are the most important factor affecting the fabrication of a uniform high-density green body. The ceramic slurry, must satisfy the following conditions to obtain a highly dense green body: (1) high solid content, (2) low viscosity, and (3) good dispersion [22–24]. A satisfactory slurry can be obtained by choosing a suitable dispersant of critical concentration and proper pH [25]. Polyelectrolytes are usually added as dispersants to enhance slurry stability and to modify the rheology in the colloidal processing of ceramics. The electrical double-layer thickness (Debye length) in a suspension, which is one of the most important processing parameters, is usually much smaller than the polymer adsorption layer thickness [26]. Other characteristic values, i.e. the Hamaker constant of the particles, the radius of the particles and the electrostatic double layer thickness, are thought to be changed by the adsorption of the polymer. Therefore, the dispersant concentration is assumed to have an extremely strong effect on the value of the zeta potential. The effect of pH and dispersant concentration on the zeta potential is the basis of this research on the cast formation of advanced ceramics.

Esposito et al. [15] reported the formation of pore-free transparent Nd:YAG ceramic with neodymia–yttria–alumina powder using the cold isostatic pressing (CIP) and slip casting (SC) methods. The aqueous slip casting of transparent YAG ceramics with commercial yttria–alumina mixed powder was discussed by Appagyeyi et al. [16]. The purpose of the present work is to explore the optimal conditions for preparing fully dense, nanostructured ceramics with neodymia–yttria–alumina powder using the slip casting method. The effort is focused on investigating the effect of pH and dispersant concentration on the zeta potential with neodymia–yttria–alumina powder. Based on a determination of the optimal parameters, the rheology of slurries with different solid content was investigated. A uniform green body with high solid content was prepared that was appropriate for the preparation of transparent Nd:YAG ceramic. The green body was thoroughly characterized in terms of its microstructure and density.

2. Experimental procedures

Homogeneous neodymia–yttria–alumina powder was purchased from Tianjin Xinchun Chemical research institute. The dispersant used in this study was an NH_4^+ salt of polyacrylic acid (NH_4PAA) (30 wt.%, Shanghai Reagents Co.). Phase identification of the commercial powder was performed by X-ray diffractometry (XRD, Advance D8, Germany) using $\text{Cu K}\alpha$ radiation ($\lambda = 1.5418 \text{ \AA}$).

A Zeta potential analyzer (Zetapals, Brookhaven Instruments Corporation, USA) was used to characterize the electrokinetic properties of the mixed powder. For the zeta potential measurement a powder suspension of 2 mg/ml concentration was prepared by dispersing the powder in deionized water under continuous magnetic stirring. The effect of pH (in the range of 7–12) on the electrokinetic properties of the mixed powder was investigated in measuring the zeta potential by adjusting the pH of the suspension with the addition of 0.1 M sodium hydroxide (NaOH) solution. The effect of adding NH_4PAA on the electrokinetic properties of the suspension was explored by measuring the zeta potential of the 2 mg/ml concentration suspension with different concentrations of NH_4PAA at a fixed pH (10.5).

Rheological measurements are typically used to characterize the behavior of fluid materials subjected to deformation strain [27], defined as the shear rate, $\dot{\gamma}$. The rheological behavior of a fluid is described by one of two flow curves: τ (shear stress) = $f(\dot{\gamma})$ or η (viscosity) = $f(\dot{\gamma})$. Highly solid-loaded mixed powder slurries (48 wt.%, 53 wt.%, 58 wt.%) with optimal pH and an additional amount of NH_4PAA were carefully prepared by adding a fixed amount of mixed powder into a fixed volume of water of optimal pH and an additional amount of NH_4PAA . The mixture was then ball milled for rheological behavior measurements. The rheological behavior was

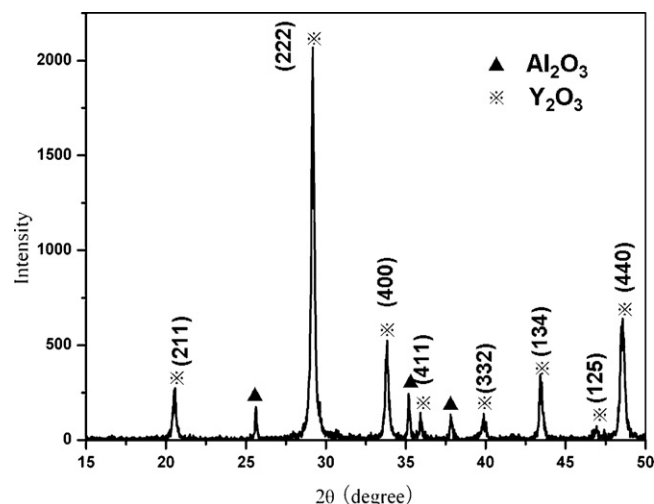


Fig. 1. XRD patterns of mixed powders.

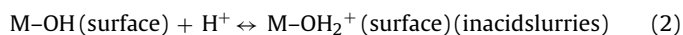
studied by measuring the viscosity and shear stress as a function of shear rate on a rheometer (HAAKE RheoStress RS75, Germany). The measurements were performed at a constant temperature of 25 °C using a cylindrical configuration.

The suspensions with the highest solids content, while retaining low viscosity, were subsequently slip cast in Plaster of Paris molds to form green bodies. The density of the formed green bodies was measured by the Archimedes method using kerosene. After being thermally etched at 1450 °C for 4 h, the fracture surfaces of the green samples and the ceramic grain boundaries were examined using field emission scanning electron microscopy (SEM, S-4800, Hitachi, Tokyo, Japan). The green body that was obtained from the optimized slurries was sintered in a vacuum furnace. Sintering was conducted at 1750 °C for 30 h in a tantalum mesh-heated vacuum furnace under $1.0 \times 10^{-3} \text{ Pa}$ vacuum. A sample (0.5 mm thick) mirror-polished on both surfaces was used to measure the optical transmittance with a Model U-4100 Spectrophotometer (Hitachi, Japan).

3. Results and discussion

X-ray diffraction (XRD) patterns of the purchased powder are shown in Fig. 1. The Y_2O_3 and Al_2O_3 phases were clearly detected but no other phase was found, which indicates that the reaction between Y_2O_3 and Al_2O_3 has not yet occurred in the starting powder. Fig. 2 shows SEM micrographs of the neodymia–yttria–alumina powder (Fig. 2(a)) and neodymia–yttria–alumina powder mixture after milling for 3 h with high purity alumina media (Fig. 2(b)). Based on visual inspection, after ball milling the powder appears to be more homogeneous than the starting powder.

Fig. 3 shows the result of ζ -potential measurements for a series of aqueous suspensions of different pH values. All the measured potential values are positive at low pH, then decrease with increasing pH, reach zero, and then become negative, and continue to decrease with further increase in the pH of the suspension. It is clear that the isoelectric point (IEP) (i.e. the pH at which the net charge on the particle surface is zero) for the as-received suspension is about pH 8.4, which is similar to the value reported in the literature [16]. This result is in agreement with the model for hydroxide groups adsorbed onto the surfaces of the particles. According to the literature, metal ions on the surface oxide layer behave as a Lewis acid [28]. In the case of aqueous slurries of oxides, a surface reaction results in the formation of amphoteric hydroxide groups, such as M-OH , which can dissociate as weak acids or bases [29]:



Below the IEP, adsorption of H^+ ions leads a positively charged surface, whereas above the IEP, the adsorption of OH^- ions produces a negatively charged surface. Pure alumina, yttria and neodymia

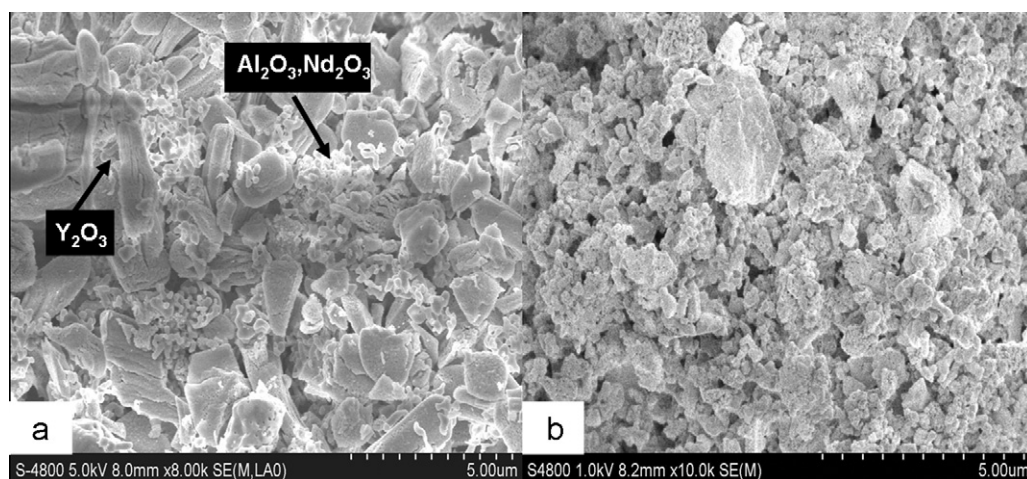


Fig. 2. SEM pictures of the as-synthesized mixed powder (a) and mixed powder after milling for 3 h (b).

particles display isoelectric points in the pH range of ~ 8.5 – 9.5 , ~ 10.5 – 11 and ~ 8.3 – 8.8 , respectively [30–32], which implies that a reasonable comparison of the surface of the powder with pure alumina and neodymia can be made.

Generally, the zeta potential depends on the amount of H^+ or OH^- adsorbed on the particle surfaces and on the thickness of the double electron layer on the particle in suspension. In the mixed powder-water system, the starting positive value of the zeta potential is due to the adsorption of protons from the solution in which they are dispersed. With the increase in pH, due to the decrease in the adsorption of protons from solution, the zeta potential gradually decreases and reaches the IEP at a pH of about 8.4. At the IEP, the rate of adsorption of H^+ approaches zero and the net adsorption of H^+ and OH^- ions on the particle surfaces are almost equal, so the zeta potential is zero. At this point, the slurry is very unstable, and agglomeration of the particles occurs even in a low load content slurry. The adsorption of OH^- on the powder surfaces from solution leads to a negative zeta potential value when the pH goes beyond the IEP. The amount of OH^- adsorbed on the surface of the nanoparticles increases with the increase in pH, which brings about an increase in the zeta potential of the particles. At pH 10.5, the amount of OH^- adsorbed on the particle surfaces reaches a maximum, and the zeta potential reaches its minimum

value (-34 mV). At this pH, the repulsive force on the particles is caused by the negative charges adsorbed on the particle surfaces, and the state is stable. To summarize, at a pH value of approximately 10.5, the particle-water system is in its most stable configuration. It is empirically generally accepted that, below the critical value of ± 30 mV, suspensions of lyophobic particles undergo changes in their dispersion state [33]. Therefore, the assessment of the properties of the suspension on the amount of dispersant is made at pH 10.5.

Fig. 4 shows the effect of concentration of the NH_4PAA (w) polymer on the zeta potential of the mixed particles in aqueous suspension with pH 10.5. The addition of NH_4PAA lowers the zeta potential of the mixed powder in suspension in conformity with other oxide slurry systems. The zeta potential decreases with an increase in the amount of NH_4PAA . After reaching a minimum value at $w=5.2$, it increases with additional amounts. The observation that dispersant addition increases the absolute value of the zeta potential indicates that anions from dissociated NH_4PAA are specifically adsorbed on the particle surface. The NH_4PAA functional groups are carboxylic acid (COO^-) groups in an aqueous solution, as illustrated below:

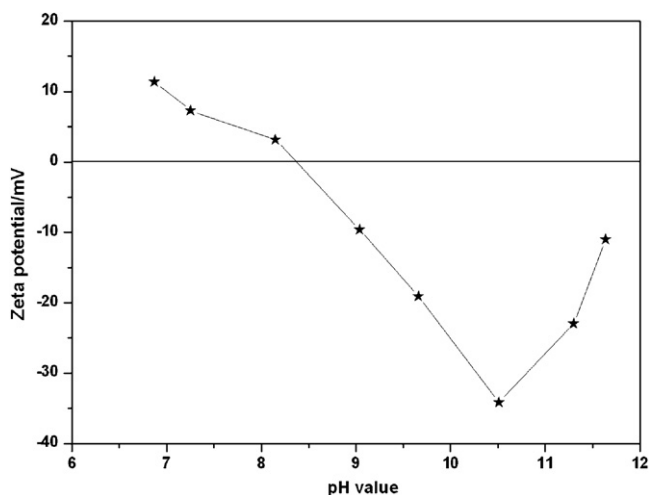


Fig. 3. Effect of pH on the ζ -potential of mixed powder in aqueous solution ($T=25^\circ C$).

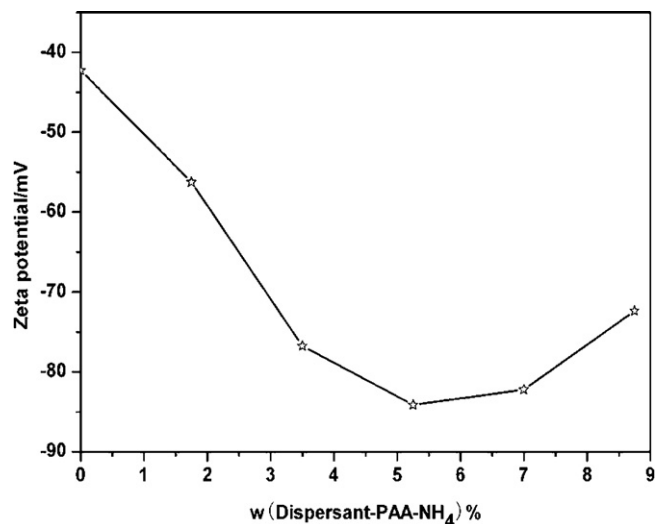
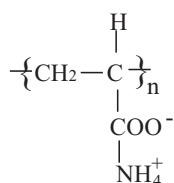


Fig. 4. Zeta potential of the slurry as a function of NH_4PAA concentrations with pH 10.5.



The ammonium carboxylate groups dissociates according to the reaction $\text{RCOONH}_4 = \text{RCOO}^- + \text{NH}_4^+$, which begins at a pH > 3.5; at pH ≥ 8.5 the polymer charge is negative with the degree of ionization approaching 1 [34]. Yu and Somasundaran [35] reported that at a pH of 10, NH_4PAA is fully ionized and adsorption is dominated by electrostatic interactions between the ionized sites on the polymer and the surface charged sites on the solid. In our experiment, the lowest zeta potential of the mixed slurry is about -85 mV when the concentration of NH_4PAA is 5.2 wt.%, which indicates that this concentration is optimal for the addition of NH_4PAA in the mixed powder–water system. At this concentration, the adsorbed polymer layer on the mixed powder is close to a monolayer. This dispersant amount is considered optimum for stabilizing the suspension. Any further addition would not be adsorbed and would negatively affect the stability of the suspension with depletion and/or flocculation. Adding dispersant beyond what gives maximum coverage of the particle surfaces can lead to an excess of dispersant in solution, which in turn would exert a detrimental effect on the rheology for two possible reasons [16]: (1) acting as a free electrolyte, the ionic strength increases and thus screens the electrostatic forces on the particles, and (2) forming a complete monolayer or even a second adsorbed layer on the surface of particles with opposite orientation, thus completely reversing the surface charge. The former may lead to depletion flocculation as a result of the osmotic pressure created by the exclusion of unadsorbed polymer chains between two approaching particles that are coated by the dispersant. The latter, on the other hand, may lead to repulsive electrosteric particle interactions at higher dispersant concentrations.

It is understandable that the behavior of the slurry also depends on the concentration of the solid phase. The rheological behavior of a mixed powder– NH_4PAA slip was studied by measuring the shear stress and viscosity at varying shear rates, while maintaining different solid content (48 wt.%, 53 wt.%, 58 wt.%) values at pH 10.5 with 5.2 wt.% dispersant, as shown in Fig. 5(a) and (b). The flow curves highlight the observation that the suspensions measured are “non-Newtonian systems”, and exhibit plastic behavior. From Fig. 5(a), it is clear that the slurry for 48 wt.% and 53 wt.% loading exhib-

Table 1

Summary of the characteristics of the microstructured suspensions prepared under different conditions.

Sample	Solid content (wt.%)	pH	Dispersant (wt.%)	Density (g/cm^3)
a	53	10.5	5.2	2.5851
b	53	12.5	5.2	2.2467
c	40	10.5	5.2	1.6649
d	40	10.5	0	Body cracks

ited characteristics close to Newtonian behavior, although a slight shear thinning was observed. This behavior is typical of a stable colloidal slurry. When the solid loading was increased to 58 wt.%, the slurries showed typical shear thinning behavior over the applied shear rate range. At the same time, the viscosity increased with increasing solid loading. The shear thinning behavior has been interpreted to be the result of the gradual breaking down of the structures formed while the fluid was in repose, indicating that a high shear stress is necessary to break them. At low shear rates, the slurry structure is close to equilibrium, and thermal motion dominates over viscous forces. At higher shear rates, the viscous forces affect the slurry structure more, causing it to become distorted, hence leading to shear thinning [36]. In addition, a low viscosity value (solid content 48 wt.%) of 15 mPa s at the maximum shear rate ($\gamma = 1000 \text{ s}^{-1}$) is observed in Fig. 5(a), thus confirming the good dispersing ability of the NH_4PAA for mixed powder aqueous slurries. From the above results, the suspensions based on solid content 48 wt.% seem to exhibit the best rheological behavior. Given the relationship between solid content and compact density, the solid content 53 wt.% slurry is considered to be the optimum.

Detailed characteristics of the suspensions prepared under a range of different conditions are summarized in Table 1. From this table, it is clear that with the various casting parameters employed, the green density is different. It should be pointed out that the green body cracked when no dispersant was added in the process of ball milling. The highest green density at 56.8% of the theoretical limit ($2.5851 \text{ g}/\text{cm}^3$) was obtained under optimum dispersion conditions. This result indicates that the addition of 5.2 wt.% of the dispersant into the suspensions with 53 wt.% solid content leads to a green body with smaller pore diameter and one that is more compact. These results are in good agreement with the theoretical discussion above.

Fig. 6 shows the microstructure of the fracture surfaces of green bodies under different conditions. The condition of the various samples is identical to those in Table 1. A well-defined and more

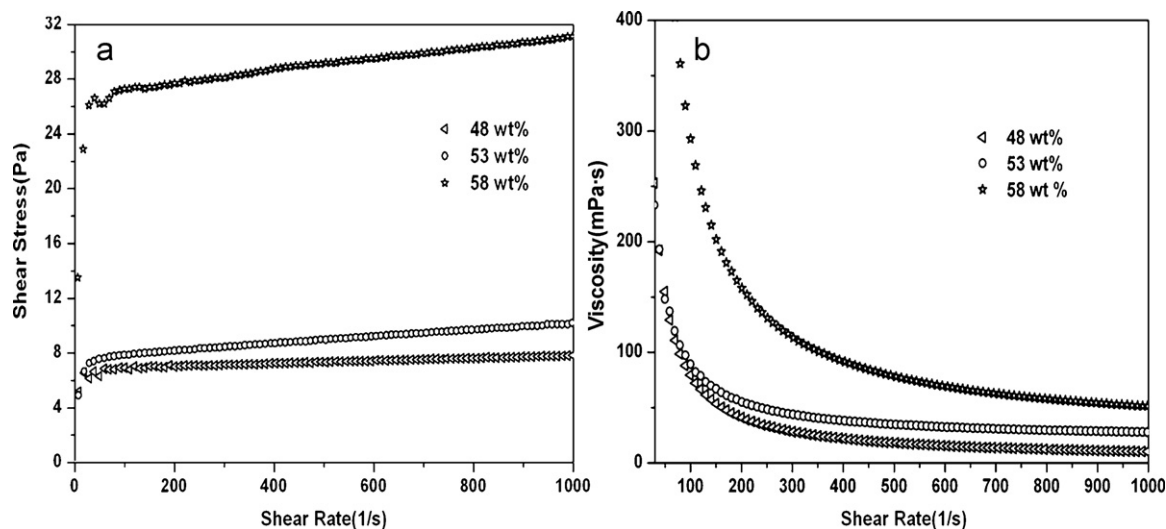


Fig. 5. Rheological behavior of concentrated (48 wt.%, 53 wt.%, 58 wt.%) suspensions at pH 10.5 with 5.2 wt.% dispersant: (a) shear stress and (b) apparent viscosity vs. shear rate.

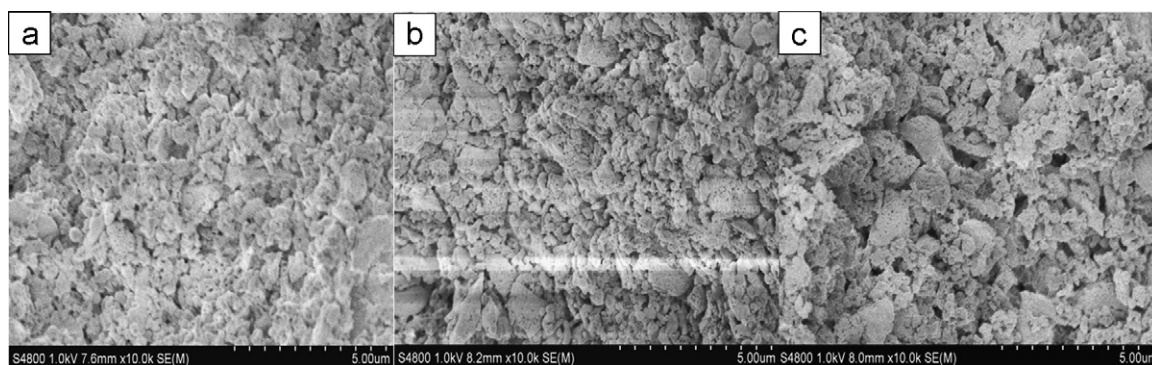


Fig. 6. SEM micrographs of fracture surfaces of slip cast green bodies under different conditions: (a) 53 wt.%, pH 10.5; (b) 53 wt.%, pH 12.5; (c) 40 wt.%, pH 10.5.

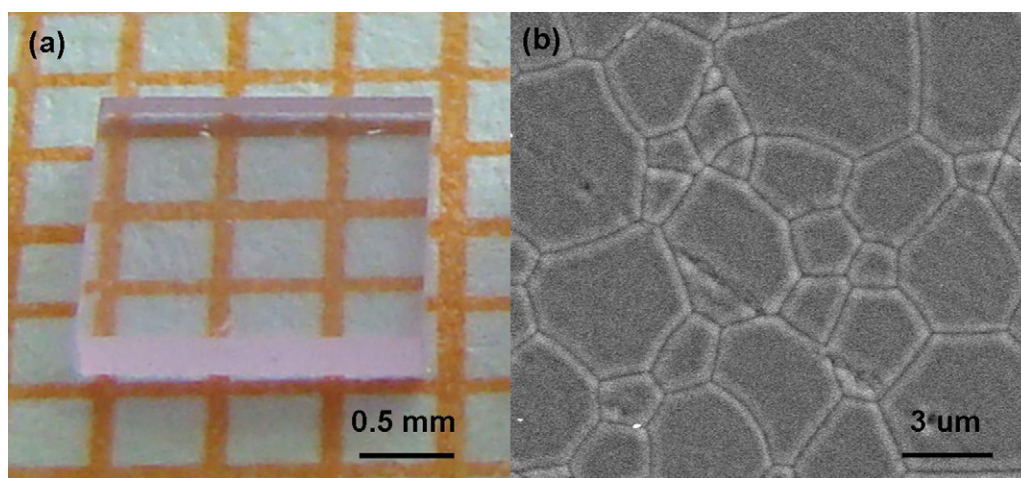


Fig. 7. Photograph (a) and SEM microstructure (b) of transparent Nd:YAG ceramic sintered at 1750 °C for 30 h in a vacuum furnace.

uniform microstructure can be observed as shown in Fig. 6(a). Some flocculation among the particles can be observed again when the pH of the slurry is further increased (Fig. 6(b)). Further pH increase renders poor slurry rheology, leading to a more inhomogeneous microstructure. More pores were observed in the green body (Fig. 6(c)), indicating that a low solid content (40 wt.%) is not sufficient to obtain a compact green body. The pH value and solid content play an important part in preparing fully dense, nanostructured ceramics with neodymia–yttria–alumina powder using the slip casting method. Comparing the microstructure of the green bodies under a range of different conditions, an obvious difference in the compact density was observed among these samples. These results are in good agreement with the density measurement of the green bodies.

Fig. 7(a) displays a photograph of the vacuum-sintered Nd:YAG ceramic sample. It can be seen that the sample is transparent. The mixed powders can be sintered to high transparency at 1750 °C by the slip casting method without SiO₂ addition [37,38] or MgO addition [39,40], which were used as sintering additives. An SEM image of the thermal-etched ceramics sample is shown in Fig. 7(b). From this figure, we can see that the materials are dense without evident pores in the sintered sample, and the microstructure is quite uniform. Most grains in the microstructure are around 5–10 μm in size.

Fig. 8 shows the straight-line light transmission curve of Nd:YAG transparent ceramic. From this curve, we can see that the optical transmittance of the sample is 72.1% at the lasing wavelength of 1064 nm, which is lower than that of single crystal Nd:YAG [41]. The characteristic absorption peak of neodymium ions at 808 nm is evident. In order to improve the optical quality of transparent

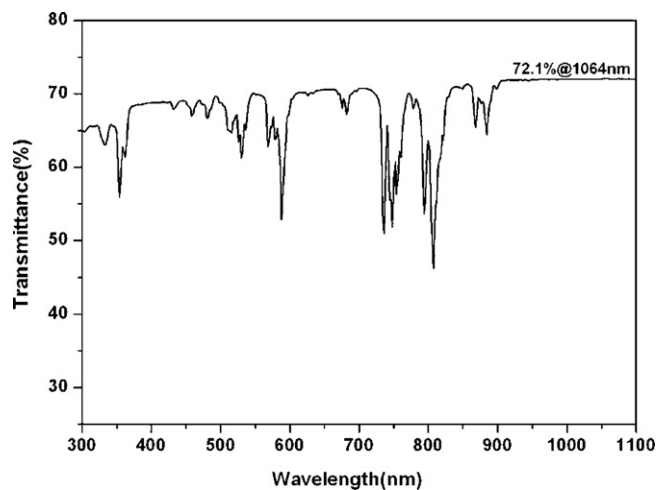


Fig. 8. Light transmission curve of Nd:YAG transparent ceramics.

ceramics prepared by this method, the effects of the sintering aids, such as TEOS alone, MgO alone, TEOS combined with MgO, on the optical quality of the ceramic will be investigated in the future.

4. Conclusions

It is revealed in the present studies that high density and homogeneous microstructure Nd:YAG ceramic green bodies can be prepared with well-dispersed neodymia–yttria–alumina particles

by using the slip casting method. The Zeta potential of mixed powders in deionized water was studied over the pH range of 7–12. Good dispersion was observed at a pH of 10.5 and at a NH_4PAA concentration of 5.2 wt.%, as revealed by a minimum in the zeta potential for the slip. The rheological behavior of the slip for different solid loading shows that slip with a solid loading of 53 wt.% exhibits near-Newtonian behavior, whereas with higher solid loading the behavior changes to a shear thinning mode. At the optimum pH value of 10.5 and at a dispersant concentration of 5.2 wt.%, a 53 wt.% solid loaded slip was successfully slip cast to produce a dense ceramic with homogeneous microstructure. Uniform and fully dense transparent Nd:YAG ceramics were obtained by sintering of compacts prepared from optimized slurries at 1750 °C in vacuum with no additional sintering aids.

Acknowledgments

This research was supported by NSFC (Nos: 50872070, 50702031, 50925205, 50990303), and the Programme of Introducing Talents of Discipline to Universities of China (111 program No. B06015), and was supported by the National Natural Science Foundation of China (Grant No. 50701002).

References

- [1] B. Cockayne, J. Less-Common Met. 144 (1985) 119–206.
- [2] Z.H. Chen, Y. Yang, Z.G. Hu, J.T. Li, S.L. He, J. Alloys Compd. 33 (2007) 328–331.
- [3] J. Lu, K. Ueda, H. Yagi, T. Yanagitani, Y. Akiyama, A.A. Kaminskii, J. Alloys Compd. 341 (2002) 220–225.
- [4] D. Hreniak, W. Strek, J. Alloys Compd. 341 (2002) 183–186.
- [5] X.L. Zhang, D. Liu, Y.H. Sang, H. Liu, J.Y. Wang, J. Alloys Compd. 502 (2010) 206–210.
- [6] T.D. Huang, B.X. Jiang, Y.S. Wu, J. Li, Y. Shi, W.B. Liu, Y.B. Pan, J.K. Guo, J. Alloys Compd. 478 (2009) L16–L20.
- [7] T.G. Deineka, A.G. Doroshenko, P.V. Mateychenko, A.V. Tolmachev, E.A. Vovk, O.M. Vovk, R.P. Yavetskiy, V.N. Baumer, D.S. Sofronov, J. Alloys Compd. 508 (2010) 200–205.
- [8] Z.H. Chen, Y. Yang, Z.G. Hu, J.T. Li, S.L. He, J. Alloys Compd. 433 (2007) 328–331.
- [9] W.X. Zhang, J. Zhou, W.B. Liu, J. Li, L. Wang, B.X. Jiang, Y.B. Pan, X.J. Cheng, J.Q. Xu, J. Alloys Compd. 506 (2010) 745–748.
- [10] L. Wen, X.D. Sun, Z.M. Xiu, S.W. Chen, C.T. Tasi, J. Eur. Ceram. Soc. 24 (9) (2004) 2681–2688.
- [11] W.B. Liu, W.X. Zhang, J. Li, H.M. Kou, Y.Q. Shen, L. Wang, Y. Shi, D. Zhang, Y.B. Pan, J. Alloys Compd. 503 (2010) 525–528.
- [12] H.X. Zhou, Q.H. Yang, J. Xu, H.J. Zhang, J. Alloys Compd. 471 (1–2) (2009) 474–476.
- [13] X. Li, Q. Li, Ceram. Int. 34 (2008) 397–401.
- [14] Y.L. Kopylov, V.B. Kravchenko, S.N. Bagayev, V.V. Shemet, A.A. Komarov, O.V. Karban, A.A. Kaminskii, Opt. Mater. 31 (5) (2009) 707–710.
- [15] L. Esposito, A. Piancastelli, J. Eur. Ceram. Soc. 29 (2) (2009) 317–322.
- [16] K.A. Appiagyei, G.L. Messing, J.Q. Dumn, Ceram. Int. 34 (5) (2008) 1309–1313.
- [17] M. Naito, Y. Fukuda, N. Yoshikawa, H. Kamiya, J. Tsubaki, J. Eur. Ceram. Soc. 17 (1997) 251–257.
- [18] Y. Hirata, Ceram. Int. 23 (1997) 93–98.
- [19] Y. Li, J. Lin, J.Q. Gao, G.J. Qiao, H.J. Wang, Mater. Sci. Eng. A 483–484 (2008) 676–678.
- [20] Y.L. Kopylov, V.B. Kravchenko, A.A. Komarov, Z.M. Lebedeva, V.V. Shemet, Opt. Mater. 29 (2007) 1236–1239.
- [21] Y.J. Hotta, N.K. Omura, K. Sato, K.J. Watari, J. Eur. Ceram. Soc. 27 (2007) 753–757.
- [22] L.B. Garrido, E.F. Agletti, J. Eur. Ceram. Soc. 21 (2001) 2259–2266.
- [23] R. Moreno, A. Salomoni, I. Stamenkovic, J. Eur. Ceram. Soc. 17 (1997) 327–331.
- [24] A. Tsetsekou, C. Agraftotis, A. Miliadis, J. Eur. Ceram. Soc. 21 (2001) 363–373.
- [25] R.R. Rao, H.N. Roopa, T.S. Kannan, Ceram. Int. 25 (1999) 223–230.
- [26] K. Lu, C.S. Kessler, R.M. Davis, J. Am. Ceram. Soc. 89 (2006) 2459–2465.
- [27] L.R. Parfitt, Dispersion of powders in liquids with special reference to pigments. Applied Science Publishers, London, U.K. 1981.
- [28] P.W. Schindler, Surface complexes at oxide-water interface. Ann Arbor Science Publishers, Ann Arbor, MI 1981.
- [29] D. Houivet, J.E. Fallah, J.M. Haussonne, J. Am. Ceram. Soc. 85 (2002) 321–328.
- [30] G.A. Parks, Chem. Rev. 65 (1965) 177–198.
- [31] R.H. Yoon, T. Salman, G. Donnay, J. Colloid Sci. 70 (1979) 483–493.
- [32] G.A. Parks, P.L. Debruyn, J. Phys. Chem. 66 (1962) 973–987.
- [33] D.H. Everett, Basic principles of colloid science. The Royal Society of Chemistry, Cambridge, 1988.
- [34] J.I.I. Cesarano, I.A. Aksay, A. Bleier, J. Am. Ceram. Soc. 71 (1988) 250–255.
- [35] X. Yu, P. Somasundaran, J. Colloid Interface Sci. 177 (1996) 283–287.
- [36] S.C. Li, Q.L. Zhang, H. Yang, D. Zou, Ceram. Int. 35 (2009) 421–426.
- [37] A. Ikesue, K. Kamata, J. Am. Ceram. Soc. 79 (1996) 1927–1933.
- [38] A. Ikesue, K. Yoshida, K. Kamata, J. Am. Ceram. Soc. 79 (1996) 507–509.
- [39] Y. Li, S. Zhou, H. Lin, X. Hou, W. Li, H. Teng, T. Jia, J. Alloys Compd. 502 (2010) 225–230.
- [40] A. Ikesue, K. kamata, K. Yoshiita, J. Am. Ceram. Soc. 79 (1996) 1921–1926.
- [41] X. Zhang, D. Liu, Y. Sang, H. Liu, J. Wang, J. Alloys Compd. 502 (2010) 206–210.